Published in final edited form as:
Invest Ophthalmol Vis Sci. 2004 August ; 45(8): 2514–2521. doi:10.1167/iovs.04-0065.

Modulating Expression of Peripherin/*rds* in Transgenic Mice: Critical Levels and the Effect of Overexpression

May Nour[1], **Xi-Qin Ding**[1], **Heidi Stricker**[1], **Steven J. Fliesler**[2,3], and **Muna I. Naash**[1]

[1]Department of Cell Biology, University of Oklahoma Health Sciences Center, Oklahoma City, Oklahoma

[2]Department of Ophthalmology, St. Louis University School of Medicine, St. Louis, Missouri

[3]Department of Pharmacological and Physiological Science, St. Louis University School of Medicine, St. Louis, Missouri

Abstract

PURPOSE—Mutations in the photoreceptor-specific protein peripherin/*rds* are associated with multiple retinal diseases. To date, attempts to achieve complete structural and functional rescue in animal models of peripherin/*rds*-induced retinal degeneration have not been successful. Gene therapy – directed approaches have been hindered by the haploinsufficiency phenotype, which dictates well-regulated expression of peripherin/*rds* protein levels.

METHODS—Using a transgenic mouse line expressing wild-type peripherin/*rds* (NMP), the authors evaluated the critical in vivo level of peripherin/*rds* needed to maintain photoreceptor structure and ERG function and assessed the consequences of peripherin/*rds* overexpression in both rods and cones by Western blot and immunoprecipitation analyses, immunohistochemistry, electron microscopy, and electroretinography. The NMP transgene included a C-terminal modification (P341Q) to facilitate detection of the transgenic protein in the presence of wild-type peripherin/*rds*, using the monoclonal antibody 3B6.

RESULTS—Peripherin/*rds* protein levels in NMP homozygotes were ~60% of wild-type levels. Western blot and immunoprecipitation analyses confirmed normal biochemical properties of the NMP protein when compared with wild-type peripherin/*rds*. Immunohistochemistry demonstrated appropriate localization of transgenic peripherin/*rds* protein to the disc rim region of photoreceptor outer segments. Total peripherin/*rds* levels in the retina were modulated by crossing NMP transgenic mice into different *rds* genetic backgrounds. A positive correlation was observed between peripherin/*rds* expression levels and the structural and functional integrity of photoreceptor outer segments. Overexpression of peripherin/*rds* caused no detectable adverse effects on rod or cone structure and function.

CONCLUSIONS—These findings may have significant implications regarding therapeutic intervention in peripherin/*rds*-associated retinal diseases.

Peripherin/*rds* (P/*rds*) is an integral membrane glycoprotein distributed along the disc rim region of rod and cone outer segments (OS) as well as adjacent to the connecting cilium at the site of disc morphogenesis.[1,2] Previous studies have highlighted its necessity in disc assembly, orientation, and physical stability and its suggested role in photoreceptor renewal.[2–4] Valuable

Corresponding author: Muna I. Naash, University of Oklahoma, Health Sciences Center, 940 S. L. Young Boulevard, BMSB 781, Oklahoma, City, OK 73104; mnaash@ouhsc.edu.

Disclosure: **M. Nour**, None; **X.-Q. Ding**, None; **H. Stricker**, None; **S.J. Fliesler**, None; **M.I. Naash**, None

insight into the structural role of P/*rds* has been provided by the *retinal degeneration slow* (*rds*) mouse,[5] in which a lack of endogenous P/*rds* protein leads to aberrant OS morphogenesis, followed by late-onset retinal degeneration.[6–9]

P/*rds* associates noncovalently with its nonglycosylated homologue Rom-1,[10–13] and in vivo and in vitro studies have shown that these interactions result in the formation of homomeric and heteromeric core complexes.[14] These complexes play a crucial role in the maintenance of OS structural integrity. However, the difference in severity of phenotype between *rds* null mutant[6–9] and Rom-1 knockout mice[15] indicates a primary and more critical role for P/*rds* in disc morphogenesis and maintenance.

More than 80 mutations in P/*rds* have been associated with retinal disease, 70% of which are single-point mutations with the remainder likely leading to a failure in protein expression. [16] The expressed phenotypes caused by these mutations in humans are heterogeneous, including retinitis pigmentosa and cone–rod dystrophy, among others.[17–20] The *rds* and transgenic mouse models have been instrumental in studying the function of P/*rds* and the disease pathogenesis caused by its loss or mutation.[1,13,21–23] These models have provided an experimental system for testing therapeutic interventions for the treatment of retinal disease associated with expression of mutant forms of P/*rds*.[24–27] In terms of therapy, P/*rds* poses a particular challenge because of a phenotype of haploinsufficiency associated with inadequate expression of the protein.[23] In the present study, we addressed two main subjects related to P/*rds* expression in rods and cones. First, we evaluated the critical levels of P/*rds* expression needed for short- and long-term maintenance of OS structure and function. Second, from a therapeutic application perspective, we assessed the effects of uniform P/*rds* overexpression on retinal morphology and ERG function. To perform our investigations, we generated transgenic mice carrying wild-type P/*rds* and mated them to $rds^{-/-}$ mice to modulate rod and cone P/*rds* levels.

MATERIALS AND METHODS

Generation of Transgenic Mice Expressing Normal Mouse P/*rds*

The transgene, a 1.6-kb full-length mouse P/*rds* cDNA, was directed to rods and cones by a 1.3-kb fragment of the human interphotoreceptor retinoid binding protein (hIRBP) promoter and included a 0.9-kb SV40 small t-intron and a polyA signal. The hIRBP promoter has been shown to direct efficient transgene expression to both rod and cone photoreceptors in mice.[28–30] Transgenic mice were generated as described[31] and were identified by polymerase chain reaction (PCR) with primers used specific for the hIRBP promoter (forward: CAGTGTCTGGCATGTAGCAGG) and the coding region of P/*rds* (reverse: GGCTTCCACTTGGCGTACTTG). *N*ormal *m*ouse *P*/*rds* (NMP) founders were mated to C57BL/6 and *rds* mice.

Animals were maintained under cyclic lighting conditions (12 light–dark, at 20 lux). Experiments were approved by Institutional Animal Care and Use Committees and conformed to the NIH Guide for Care and Use of Laboratory Animals and the ARVO Statement for Use of Animals in Ophthalmic and Vision Research.

Scotopic and Photopic Electroretinography

ERG testing was performed as described.[32] In brief, dark-adapted mice were administered an intramuscular injection of 85 mg/kg ketamine (Fort Dodge Animal Health; Fort Dodge, IA) and 14 mg/kg xylazine (The Butler Company; Columbus, OH). After anesthesia, vibrissae were trimmed and the eyes were dilated with 2.5% phenylephrine (Akorn, Inc., Decatur, IL). Electroretinograms (ERGs) were recorded with a stainless steel wire contacting the corneal

surface through a layer of 2.5% methylcellulose, and animals were placed on a regulated heating pad throughout the experiment. Needle electrodes in the cheek and tail of the animals served as reference and ground leads, respectively. Responses were differentially amplified (half bandpass, 1–4000 Hz), averaged, and stored with signal averaging system (Compact 4; Nicolet Instrument Corp., Madison, WI). For the assessment of rod photoreceptor function (scotopic ERG), a strobe flash stimulus was presented to the dark-adapted, dilated eyes in the Ganzfeld (GS-2000; Nicolet Instrument Corp.) with a 137-cd · s/m^2) flash intensity. The amplitude of the a-wave was measured from the prestimulus baseline to the a-wave trough, whereas the amplitude of the b-wave was measured from the a-wave trough to the b-wave peak. For evaluation of cone function (photopic ERG), animals were light adapted for 5 minutes under a light intensity of 29.0285 cd/m^2. A strobe flash stimulus was presented to the light-adapted, dilated eyes in the Ganzfeld with a 77-cd · s/m^2) flash intensity. The amplitude of the cone b-wave was measured from the a-wave trough to the b-wave peak.

Analysis of variance (ANOVA) and post hoc statistical tests using Bonferroni's pair-wise comparisons were used to determine the significance of differences in ERG responses (Prism ver. 3.02; GraphPad, San Diego, CA).

Histology at the Light and Electron Microscopy Level

Enucleated eyes were fixed and sectioned as described.[33] After sacrifice, the superior cornea was marked with a flaming needle before enucleation and a slit was made posterior to the cornea before a 1 hour fixation in freshly prepared 0.1 M sodium phosphate buffer (pH 7.4), containing 2.5% glutaraldehyde, 2.0% paraformaldehyde, and 0.025% $CaCl_2$. The cornea and lens were then removed, and fixation was continued overnight. Fixed eyecups were rinsed twice for 10 minutes each in 0.1 M sodium cacodylate buffer (pH 7.4), containing 0.025% $CaCl_2$, postfixed for 1 hour in 1% OsO_4 in 0.1 M sodium cacodylate, at room temperature, in the dark, then rinsed twice in cacodylate buffer and once in distilled water (DW).

Eyecups were dehydrated through a graded ethanol series followed by propylene oxide, infiltrated for 24 hours with Spurr resin, embedded in BEEM capsules (Beem Company, Bronx, NY) and polymerized at 70°C for 48 hours. Sectioning was performed on a microtome (Ultracut E; Reichert-Jung, Vienna Austria) equipped with glass and diamond (Diatome, Biel, Switzerland) knives. Semithin (0.75 μm) sections were stained with 1% toluidine blue in 1% sodium borate. Thin (silver) sections were collected on copper 75/300 mesh grids, poststained with 2% uranyl acetate (aqueous) and lead citrate (Reynolds), and photographed by electron microscope (100CX; JEOL, Tokyo, Japan) at an accelerating voltage of 60 kV. Sections were viewed and photographed with a photomicroscope (BH-2; Olympus Corp. of America, Lake Success, NY) in the autoexpose mode, using 20× or 60× objectives.

Immunofluorescence Labeling

Enucleated eyes were fixed as previously described[23] and evaluated using anti-P/*rds* mAb 3B6 (1:5; Robert Molday, University of British Columbia, Vancouver, BC, Canada) and anti-human-blue opsin (1:3000; Jeremy Nathans, Johns Hopkins University, Baltimore, MD).[34] The anti-P/*rds* mAb 3B6 has the ability to exclusively recognize C-terminal–modified, but not endogenous, P/*rds* protein. Sections were incubated overnight at 4°C with primary antibodies followed by three phosphate-buffered saline (PBS) rinses, incubation with biotinylated FITC secondary antibody (1:100, 30 minutes), and finally three PBS washes. Images were captured with either an epifluorescence (Axioscope; Carl Zeiss Meditec, Jena, Germany) or a confocal (Leica TCS Sp2; Leica Microsystems, Wetzlar, Germany) microscope.

Immunoprecipitation and Immunoblot Analysis

Rabbit polyclonal antibodies against residues 331–346 and 336–351 of the P/*rds* (*rds*-C-term Ab) and Rom-1 carboxyl termini (Rom-1-C-term Ab), respectively, were used for immunoprecipitation (IP) and immunoblot analyses. The polyclonal anti-P/*rds* antibody has the ability to recognize both endogenous and the C-terminal–modified P/*rds*. Dissected retinas were homogenized on ice, solubilized for 1 hour at 4°C in solubilization buffer (50 mM Tris-HCl, [pH 7.5], 100 mM NaCl, 5 mM EDTA, 1% Triton X-100, 0.05% SDS, 2.5% glycerol, and 1.0 mM phenylmethylsulfonyl fluoride), and centrifuged at 100,000*g* for 30 minutes. The supernatants were collected for determination of protein concentration, IP, and immunoblot analyses. For IP, retinal extracts (200 μg protein) were incubated in solubilization buffer with polyclonal anti-P/*rds* antibody (1:100 dilution) or anti-Rom-1 antibody (1: 100) and protein A-Sepharose beads (Sigma-Aldrich, St. Louis, MO) in a volume of 200 μL at 4°C for 4 hours. After adsorption, the beads were washed with solubilization buffer three times (500 μL for each wash), and bound proteins were eluted with 2× sample buffer, followed by gel electrophoresis and immunoblot with anti-P/*rds* or anti-Rom-1 antibodies.

RESULTS

NMP Transgenic Protein Expression and Localization

To exclusively recognize the NMP product by mAb 3B6, we introduced a P341Q modification into the transgene.[2] Glutamine at position 341 is the only residue of the 3B6 antigenic site shared by human, bovine, and rat P/*rds*, but replaced by a proline in the mouse. This modification was performed by oligonucleotide-directed mutagenesis (CCG→CAA).

Seven NMP lines were generated and characterized for site of integration, level of expression, and localization of the transgene product. The highest expresser was used to conduct all experiments described in this study. NMP mice were crossed onto an $rds^{-/-}$ background to quantify transgenic protein levels. Polyclonal anti-P/*rds* antibody, which recognizes both transgenic and endogenous proteins, was used to detect P/*rds*. No P/*rds* signal was found in the retinas of $rds^{-/-}$ mice (Fig. 1A, left). Densitometric analysis of four independent immunoblots revealed the level of NMP protein obtained from homozygous retinas in the $rds^{-/-}$ background to be ~60% of wild-type P/*rds* (Fig. 1A, right). Actin was used as an internal control and showed comparable levels in all samples examined (Fig. 1A, left).

Figure 1B, top, demonstrates the ability of the mAb 3B6 to recognize only rat and NMP protein, but not mouse P/*rds*. Double-labeling with mAb 3B6 and anti-blue opsin antibody confirmed the presence of NMP protein in cone OS (Fig. 1B, overlay in the bottom panel). Labeling was restricted to the OS and no immunofluorescent signal was detected in other retinal layers. Laser deconvolution microscopy (Fig. 1C) was used to demonstrate appropriate localization of the NMP protein in OS disc rim regions. Double-staining with mAb 3B6 and anti-blue opsin antibodies confirms localization of NMP to cone OS rims (Fig. 1C, overlay).

Biochemical Properties of the NMP Protein

To evaluate the effect of the C-terminal P341Q modification on the characteristics of the protein, Western blot analysis was performed under reducing and nonreducing conditions using retinal extracts from $NMP^{+/+}/rds^{-/-}$ and wild-type mice. Blots were then probed with P/*rds* and Rom-1 antibodies (Fig. 2A). Under reducing conditions, the major P/*rds* band migrated at the expected monomer position (~36 kDa)[35] with a small portion at the dimer position (~70 kDa) in retinal samples from both NMP and wild-type mice (Fig. 2A, top left). Under nonreducing conditions, dimers and higher-order oligomers were detected in both types of retinas (Fig. 2A, top right). Appearance of the dimer form of P/*rds* under reducing conditions reflects an incomplete reduction of the protein. No P/*rds* signal was detected in retinal extracts

from *rds*$^{-/-}$ mice. The comparable migration pattern of the NMP protein under both reducing and nonreducing conditions suggests that the P341Q modification in NMP has no effect on the ability of the protein to form dimers and higher-order oligomers.

We examined the expression and migration patterns of Rom-1 under reducing and nonreducing conditions from NMP retinas. Under reducing conditions, Rom-1 migrated as a monomer (~36 kDa)[11] in retinal samples from both wild-type and NMP$^{+/+}$/*rds*$^{-/-}$ mice (Fig. 2A, bottom left). Under nonreducing conditions, monomers, dimers and higher-order forms of Rom-1 were observed (Fig. 2A, bottom right). The migration pattern of Rom-1 in NMP retinal extracts was similar to that observed in wild-type extracts, indicating a lack of negative effect of the P341Q modification on Rom-1 expression. Moreover, levels of Rom-1 in *rds*$^{-/-}$ retinal extracts were significantly reduced compared with that in both wild-type and NMP extracts (Fig. 2A, bottom), suggesting that the expression or stability of Rom-1 is dependent on the presence of P/*rds* and is restored in the presence of NMP protein.

The association between P/*rds* and Rom-1 was further assessed by reciprocal co-IP analysis. The similarity in pattern of association between wild-type and NMP$^{+/+}$/*rds*$^{-/-}$ retinas suggests that the P341Q modification does not alter the ability of P/*rds* to interact with Rom-1 (Fig. 2B). Retinal samples from *rds*$^{-/-}$ mice were included as a negative control (Fig. 2B).

NMP Protein Mediates Functional and Structural Rescue of the *rds*$^{-/-}$ Retina

To test the ability of the NMP protein to build and maintain OS in the absence of endogenous P/*rds*, homozygous NMP mice were generated in an *rds*$^{-/-}$ background. In the absence of endogenous P/*rds*, *rds*$^{-/-}$ mice show no scotopic or photopic ERG response (Figs. 3A–C). Scotopic a-wave amplitudes correlated positively with P/*rds* levels in NMP$^{+/+}$/*rds*$^{-/-}$ and *rds*$^{+/-}$ mice, exhibiting a proportionate restoration of rod function (Figs. 3A, 3B). At this age, no differences in cone function were detected between NMP$^{+/+}$/*rds*$^{-/-}$ and *rds*$^{+/-}$ mice; both groups showed photopic b-wave amplitudes comparable to those of wild-type mice (Fig. 3C). Structurally, NMP$^{+/+}$/*rds*$^{-/-}$ retinas (60% of wild type) showed disorganized and swirl-like OS formation at the EM level, albeit to a lesser degree than that in r*ds*$^{+/-}$ retinas (50% of wild type) and contained relatively more OS material than did *rds*$^{+/-}$ retinas (data not shown). This finding correlates well with the additional 10% of P/*rds* in NMP$^{+/+}$/*rds*$^{-/-}$ when compared with *rds*$^{+/-}$ retinas.

Critical Level of P/*rds* Needed to Maintain Photoreceptor Structure and Function

Because haploinsufficiency phenotype associates with the loss of one P/*rds* allele,[23] we assessed the critical level of P/*rds* (in excess of 50%) necessary to maintain OS morphology and function. NMP$^{+/-}$ animals were generated on an *rds*$^{+/-}$ background, with a total amount of P/*rds* equivalent to 80% of wild type. These animals were evaluated for resolution of functional and structural defects in *rds*$^{+/-}$ mice. The 30% increase in P/*rds* in 1-month-old NMP$^{+/-}$/*rds*$^{+/-}$ relative to age-matched *rds*$^{+/-}$ retinas was evident by blot analysis (Fig. 4A). At this age, NMP$^{+/-}$/*rds*$^{+/-}$ mice showed scotopic and photopic ERG amplitudes comparable to those of wild-type mice and were considerably improved when compared with *rds*$^{+/-}$ mice (data not shown). To assess the long-term impact of this level of P/*rds* on retinal function and structure, NMP$^{+/-}$/*rds*$^{+/-}$ mice were examined at 7 months of age. A significant increase ($P < 0.001$) was detected in scotopic a-wave amplitudes, indicating improved rod function relative to age-matched *rds*$^{+/-}$ mice (Fig. 4B). Furthermore, improvement in photopic ERG responses was also significant ($P < 0.05$) in NMP$^{+/-}$/*rds*$^{+/-}$ mice relative to *rds*$^{+/-}$ (Fig. 4C). The enhancement in retinal function afforded by the increase in P/*rds* was also detected on a structural level. Retinal histology showed a considerable improvement in OS structure and length in NMP$^{+/-}$/*rds*$^{+/-}$ transgenics when compared with *rds*$^{+/-}$ mice (Fig. 4D, top). This amelioration of OS integrity was accompanied by a preservation of two to three rows of

photoreceptor nuclei. Examination of these retinas by EM confirmed the marked ultrastructural rescue of OSs (Fig. 4D, bottom). When compared with the swirl-like OSs in *rds*$^{+/-}$ retinas (50% of wild-type), exacerbated at 7-months of age, NMP$^{+/-}$/*rds*$^{+/-}$ retinas (80% of wild type) showed a remarkable, although incomplete, restoration of OS alignment and structure (Fig. 4D, bottom).

Effects of P/*rds* Overexpression

To determine the effects of P/*rds* overexpression on retinal function and structure, animals homozygous for the NMP transgene were generated on a wild-type P/*rds* background (NMP$^{+/+}$/+/+). Blot analysis (Fig. 5A) revealed ~45% to 50% overexpression of P/*rds* above wild type. Retinal ERG function was first evaluated at 1 month and its assessment continued up to 7+ months of age in mice overexpressing P/*rds.* Scotopic (Fig. 5B) and photopic (Fig. 5C) ERG wave amplitudes were not significantly altered in NMP$^{+/+}$/+/+ mice, compared with age-matched wild-type mice. Concomitantly, no histologic abnormalities were found in retinas of 4-month-old mice overexpressing P/*rds* (Fig. 5D, top). At light and EM levels, no histologic or ultrastructural abnormalities or loss of photoreceptors were detected in NMP$^{+/+}$/+/+ mice (Fig. 5D).

DISCUSSION

The loss of one allele of P/*rds* has been described to correlate with a haploinsufficiency phenotype, which presents with an abnormality in OS morphology and an early-onset deficiency in rod function, followed by a decline in cone function and a slow rate of photoreceptor degeneration.[23] Since then, studies have attempted to define more clearly the intermediate levels (50%–100%) of P/*rds* required to sustain rod photoreceptor function. [13, 27] The present study complements previous findings as the first to address the differential effects of P/*rds* modulation on both rod and cone photoreceptors in vivo. Transgenic mice expressing a modified wild-type mouse P/*rds* were used to evaluate the critical level of P/*rds* necessary for short- and long-term maintenance of OS structure and function. Moreover, we systematically evaluated the effects of P/*rds* overexpression on both photoreceptor cell types. We distinguished between the transgenic and endogenous proteins by C-terminal modification (P341Q), which allowed for exclusive recognition of the transgene product by mAb 3B6 and confirmed appropriate localization of the NMP protein to both rod and cone photoreceptor discs.[2] Biochemically, the transgenic protein was shown to interact with itself as well as with Rom-1 in a pattern identical with the endogenous P/*rds* protein.

Levels of P/*rds* resulting from each NMP transgenic allele equated to 60% of one wild-type allele. In the absence of endogenous P/*rds*, mice homozygous for the NMP transgene (60% of wild-type) were able to build OSs and recover ~60% of rod function when compared with *rds*$^{-/-}$ mice. Relative to *rds*$^{+/-}$ retinas (50% of wild-type), NMP$^{+/+}$/*rds*$^{-/-}$ retinas showed an improvement in OS structure and rod function, positively correlating with the 10% increase in P/*rds* level. In agreement with our previous findings,[23] we also observed that, unlike rods, cones are able to retain wild-type levels of ERG function at an early age with as little as 50% P/*rds* protein. It is likely that structural differences between rods and cones, in particular shorter OS length and continuous disc membrane structure of cones, account for this finding. We showed that 80% of wild-type P/*rds* was sufficient to support both normal rod and cone ERG amplitudes and normal OS structures, when compared with *rds*$^{+/-}$ retinas (50% of wild-type). In the long term, NMP$^{+/-}$/*rds*$^{-/-}$ (80% of wild-type) retinas showed a remarkable ability to maintain OS morphology, despite infrequent abnormalities, accompanied by significantly improved rod function, compared with *rds*$^{+/-}$ retinas which showed gross abnormality in OS structure and dramatically reduced rod function. Early on only a 50% level of P/*rds* is necessary for cone function, and its declines with age. This reduction in cone function may be attributed

to the previously suggested cone–rod interdependence.[36] It is worthwhile to note that, at 7 months of age, the 30% increase in P/*rds* expression afforded by the addition of one allele of the NMP transgene to the *rds*$^{+/-}$ retina not only improved rod function, but more important, it prevented age-dependent deterioration in cone photoreceptor function. This is of particular clinical significance in halting the progression of cone degeneration in cases of macular disease. These results also agree with the hypothesis that prolonging rod survival leads to a prolonged survival of cones.[37,38]

A pertinent issue the design of therapeutic strategies for the treatment of P/*rds*-associated retinal diseases is the effect of P/*rds* overexpression on photoreceptor structure and function. Using NMP transgenics, we overexpressed P/*rds* in rods and cones at a level 50% above wild type. Overexpression of P/*rds* has been suggested by Sarra et al.[26] to be detrimental to photoreceptor survival. However, neither quantitation of P/*rds* overexpression nor immunohistochemical evidence linking virally mediated expression of P/*rds* with retinal cell death was provided by that study. Although overexpression of opsin has been shown to induce photoreceptor cell death,[33]in our study, this was not the case for P/*rds*. We ensured uniform overexpression of P/*rds* in both rods and cones and showed that additional P/*rds* protein causes neither functional nor structural defects up to 7 months of age, the latest time examined.

In summary, this study is the first to define comprehensively the critical levels of P/*rds* needed in vivo to maintain long-term OS structure and function, as well as to demonstrate the lack of detectable deleterious effects resulting from P/*rds* overexpression. These findings are likely to be of value in development of gene therapy interventions in P/*rds*-associated retinal disease.

Acknowledgments

The authors thank Chibo Li for transgene construction; Alexander Quiambao, Ming Cheng, and Barbara Nagel for technical assistance; and Muayyad R. Al-Ubaidi, and Rafal Farjo for helpful comments on the manuscript.

Supported by the National Eye Institute Grants EY-10609 (MIN) and EY-07361 (SJF), and Core Grant for Vision Research (EY-12190); the Foundation Fighting Blindness (MIN); and Research to Prevent Blindness (MIN, SJF).

References

1. Connell GJ, Molday RS. Molecular cloning, primary structure, and orientation of the vertebrate photoreceptor cell protein peripherin in the rod outer segment disk membrane. Biochemistry 1990;29:4691–4698. [PubMed: 2372552]
2. Molday RS, Hicks D, Molday L. Peripherin: a rim-specific membrane protein of rod outer segment discs. Invest Ophthalmol Vis Sci 1987;28:50–61. [PubMed: 2433249]
3. Boesze-Battaglia K, Goldberg AF. Photoreceptor renewal: a role for peripherin/rds. Int Rev Cytol 2002;217:183–225. [PubMed: 12019563]
4. Wrigley JD, Ahmed T, Nevett CL, et al. Peripherin/rds influences membrane vesicle morphology. Implications for retinopathies. J Biol Chem 2000;275:13191–13194. [PubMed: 10747861]
5. van Nie R, Ivanyi D, Demant P. A new H-2-linked mutation, rds, causing retinal degeneration in the mouse. Tissue Antigens 1978;12:106–108. [PubMed: 705766]
6. Jansen HG, Sanyal S. Development and degeneration of retina in rds mutant mice: electron microscopy. J Comp Neurol 1984;224:71–84. [PubMed: 6715580]
7. Sanyal S, Jansen HG. Absence of receptor outer segments in the retina of rds mutant mice. Neurosci Lett 1981;21:23–26. [PubMed: 7207866]
8. Sanyal S, De Ruiter A, Hawkins RK. Development and degeneration of retina in rds mutant mice: light microscopy. J Comp Neurol 1980;194:193–207. [PubMed: 7440795]
9. Cohen AI. Some cytological and initial biochemical observations on photoreceptors in retinas of rds mice. Invest Ophthalmol Vis Sci 1983;24:832–843. [PubMed: 6862791]

10. Moritz OL, Molday RS. Molecular cloning, membrane topology, and localization of bovine rom-1 in rod and cone photoreceptor cells. Invest Ophthalmol Vis Sci 1996;37:352–362. [PubMed: 8603840]
11. Loewen CJ, Molday RS. Disulfide-mediated oligomerization of Peripherin/Rds and Rom-1 in photoreceptor disk membranes: implications for photoreceptor outer segment morphogenesis and degeneration. J Biol Chem 2000;275:5370–5378. [PubMed: 10681511]
12. Goldberg AF, Molday RS. Subunit composition of the peripherin/rds-rom-1 disk rim complex from rod photoreceptors: hydrodynamic evidence for a tetrameric quaternary structure. Biochemistry 1996;35:6144–6149. [PubMed: 8634257]
13. Kedzierski W, Bok D, Travis GH. Transgenic analysis of rds/peripherin N-glycosylation: effect on dimerization, interaction with rom1, and rescue of the rds null phenotype. J Neurochem 1999;72:430–438. [PubMed: 9886097]
14. Goldberg AF, Moritz OL, Molday RS. Heterologous expression of photoreceptor peripherin/rds and Rom-1 in COS-1 cells: assembly, interactions, and localization of multisubunit complexes. Biochemistry 1995;34:14213–14219. [PubMed: 7578020]
15. Clarke G, Goldberg AF, Vidgen D, et al. Rom-1 is required for rod photoreceptor viability and the regulation of disk morphogenesis. Nat Genet 2000;25:67–73. [PubMed: 10802659]
16. Lam BL, Vandenburgh K, Sheffield VC, et al. Retinitis pigmentosa associated with a dominant mutation in codon 46 of the peripherin/RDS gene (arginine-46-stop). Am J Ophthalmol 1995;119:65–71. [PubMed: 7825692]
17. Apfelstedt-Sylla E, Theischen M, Ruther K, et al. Extensive intrafamilial and interfamilial phenotypic variation among patients with autosomal dominant retinal dystrophy and mutations in the human RDS/peripherin gene. Br J Ophthalmol 1995;79:28–34. [PubMed: 7880786]
18. Fossarello M, Bertini C, Galantuomo MS, et al. Deletion in the peripherin/RDS gene in two unrelated Sardinian families with autosomal dominant butterfly-shaped macular dystrophy. Arch Ophthalmol 1996;114:448–456. [PubMed: 8602784]
19. Zhang K, Garibaldi DC, Li Y, et al. Butterfly-shaped pattern dystrophy: a genetic, clinical, and histopathological report. Arch Ophthalmol 2002;120:485–490. [PubMed: 11934323]
20. Ekstrom U, Ponjavic V, Abrahamson M, et al. Phenotypic expression of autosomal dominant retinitis pigmentosa in a Swedish family expressing a Phe-211-Leu variant of peripherin/RDS. Ophthalmic Genet 1998;19:27–37. [PubMed: 9587927]
21. Kedzierski W, Lloyd M, Birch DG, et al. Generation and analysis of transgenic mice expressing P216L-substituted rds/peripherin in rod photoreceptors. Invest Ophthalmol Vis Sci 1997;38:498–509. [PubMed: 9040483]
22. Kedzierski W, Nusinowitz S, Birch D, et al. Deficiency of rds/peripherin causes photoreceptor death in mouse models of digenic and dominant retinitis pigmentosa. Proc Natl Acad Sci USA 2001;98:7718–7723. [PubMed: 11427722]
23. Cheng T, Peachey NS, Li S, et al. The effect of peripherin/rds haploinsufficiency on rod and cone photoreceptors. J Neurosci 1997;17:8118–8128. [PubMed: 9334387]
24. Ali RR, Sarra GM, Stephens C, et al. Restoration of photoreceptor ultrastructure and function in retinal degeneration slow mice by gene therapy. Nat Genet 2000;25:306–310. [PubMed: 10888879]
25. Bok D, Yasumura D, Matthes MT, et al. Effects of adeno-associated virus-vectored ciliary neurotrophic factor on retinal structure and function in mice with a P216L rds/peripherin mutation. Exp Eye Res 2002;74:719–735. [PubMed: 12126945]
26. Sarra GM, Stephens C, de Alwis M, et al. Gene replacement therapy in the retinal degeneration slow (rds) mouse: the effect on retinal degeneration following partial transduction of the retina. Hum Mol Genet 2001;10:2353–2361. [PubMed: 11689482]
27. Schlichtenbrede FC, MacNeil A, Bainbridge JW, et al. Intraocular gene delivery of ciliary neurotrophic factor results in significant loss of retinal function in normal mice and in the Prph2Rd2/Rd2 model of retinal degeneration. Gene Ther 2003;10:523–527. [PubMed: 12621456]
28. Liou GI, Matragoon S, Yang J, et al. Retina-specific expression from the IRBP promoter in transgenic mice is conferred by 212 bp of the 5′-flanking region. Biochem Biophys Res Commun 1991;181:159–165. [PubMed: 1958183]

29. Tan E, Ding XQ, Saadi A, et al. Expression of cone-photoreceptor-specific antigens in a cell line derived from retinal tumors in transgenic mice. Invest Ophthalmol Vis Sci 2004;45:764–768. [PubMed: 14985288]
30. Quiambao AB, Tan E, Chang S, et al. Transgenic Bcl-2 expressed in photoreceptor cells confers both death-sparing and death-inducing effects. Exp Eye Res 2001;73:711–721. [PubMed: 11747371]
31. Naash MI, Hollyfield JG, Al Ubaidi MR, et al. Simulation of human autosomal dominant retinitis pigmentosa in transgenic mice expressing a mutated murine opsin gene. Proc Natl Acad Sci USA 1993;90:5499–5503. [PubMed: 8516292]
32. Li C, Cheng M, Yang H, et al. Age-related changes in the mouse outer retina. Optom Vis Sci 2001;78:425–430. [PubMed: 11444632]
33. Tan E, Wang Q, Quiambao AB, et al. The relationship between opsin overexpression and photoreceptor degeneration. Invest Ophthalmol Vis Sci 2001;42:589–600. [PubMed: 11222515]
34. Chiu MI, Nathans J. A sequence upstream of the mouse blue visual pigment gene directs blue cone-specific transgene expression in mouse retinas. Vis Neurosci 1994;11:773–780. [PubMed: 7918227]
35. Li C, Ding XQ, O'Brien J, et al. Molecular characterization of the skate peripherin/rds gene: relationship to its orthologues and paralogues. Invest Ophthalmol Vis Sci 2003;44:2433–2441. [PubMed: 12766040]
36. Mohand-Said S, Hicks D, Leveillard T, et al. Rod-cone interactions: developmental and clinical significance. Prog Retin Eye Res 2001;20:451–467. [PubMed: 11390256]
37. Mohand-Said S, Hicks D, Dreyfus H, et al. Selective transplantation of rods delays cone loss in a retinitis pigmentosa model. Arch Ophthalmol 2000;118:807–811. [PubMed: 10865319]
38. Mohand-Said S, Hicks D, Simonutti M, et al. Photoreceptor transplants increase host cone survival in the retinal degeneration (rd) mouse. Ophthalmic Res 1997;29:290–297. [PubMed: 9323720]

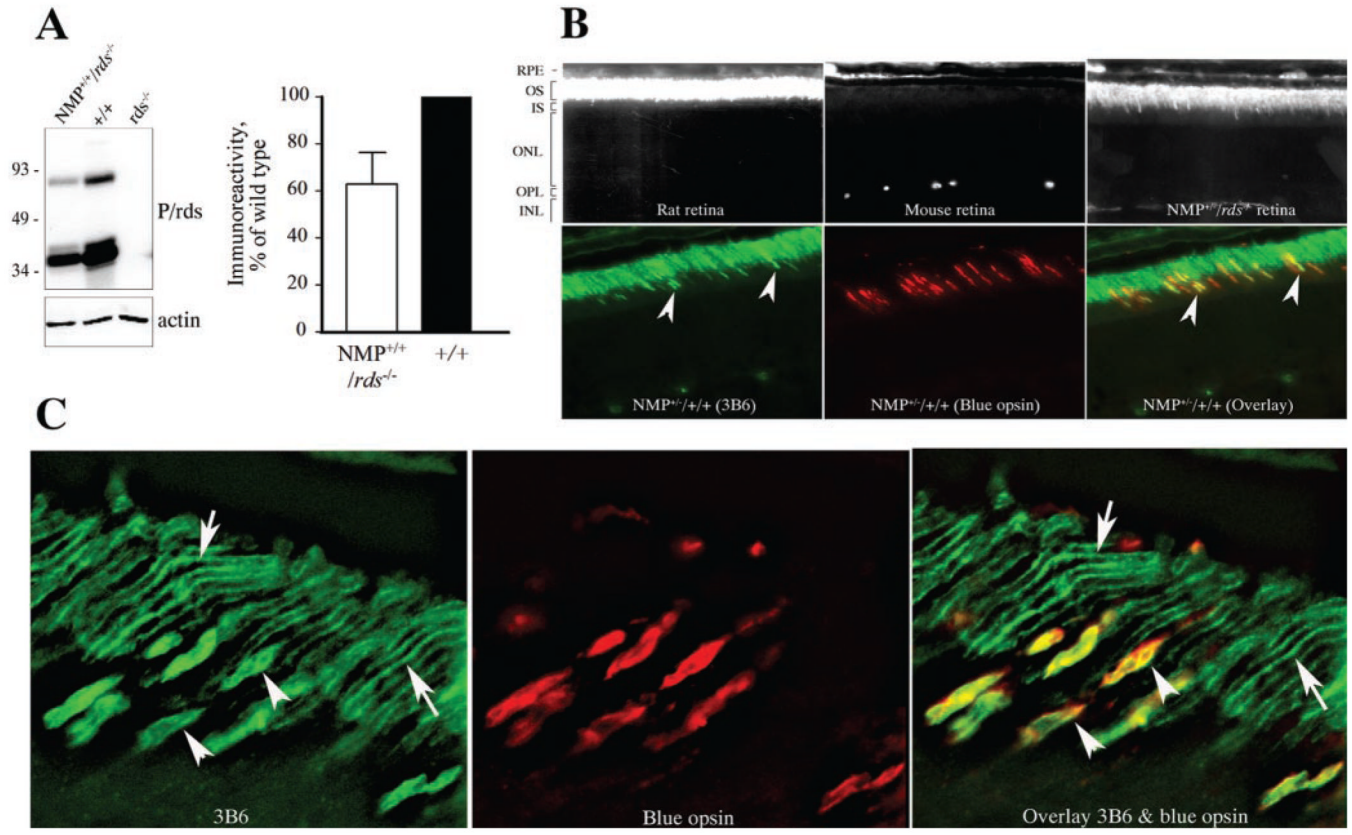

FIGURE 1.

NMP protein levels and OS localization. (**A**) Immunoblot analysis of retinal extracts from NMP$^{+/+}$/*rds*$^{-/-}$, wild-type (+/+), and *rds*$^{-/-}$ mice. Note the expected absence of P/*rds* immunoreactivity in the *rds*$^{-/-}$ retinal extract. Densitometric measurements of four independent blots are shown and were used to assess levels of NMP protein at 60% of endogenous P/*rds*. (**B**) C-terminal P431Q modification allowed immunofluorescent recognition of the NMP protein by 3B6 antibody. *Top*: ability of mAb 3B6 to recognize rat P/*rds* and NMP, but not endogenous mouse P/*rds*. Positively labeled retinal sections (rat and NMP) show mAb 3B6-staining in OS. *Bottom*: NMP retinal sections stained with both mAb 3B6 and anti-blue cone opsin antibodies, demonstrating colocalization of immunofluorescent signals. *Arrowheads*: localization to cone OS. (**C**) At higher magnification, single staining with mAb 3B6 and double staining with mAb 3B6 and anti-blue cone opsin antibodies further confirmed appropriate localization of the NMP protein to the OS disc rims of both rods (*arrows*) and cones (*arrowheads*).

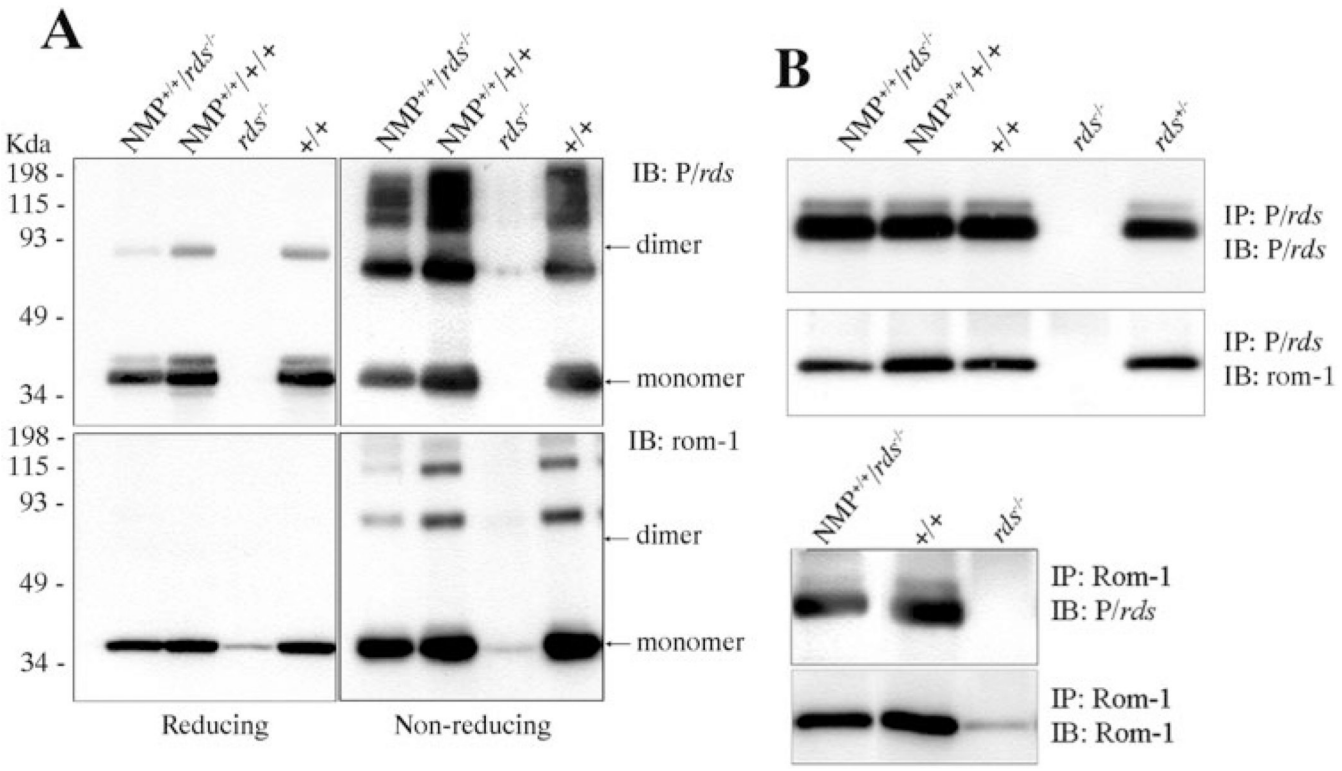

FIGURE 2.

Biochemical properties of the NMP protein. (**A**) Blot analysis of NMP protein under reducing and nonreducing conditions. Under reducing conditions, the major band of P/*rds* (*top left*) migrated as a monomer, with lesser amounts corresponding to the dimer also detected, whereas Rom-1 migrated as a monomer (*lower left*) in retinal samples from both NMP and wild-type mice. Under nonreducing conditions, dimer and higher-order oligomers of P/*rds* (*top right*) and Rom-1 (*bottom right*) were predominant. (**B**) Reciprocal Co-IP using anti-P/*rds* (*top*) and anti-Rom-1 (*bottom*) antibodies showing a comparable pattern of association between P/*rds* and Rom-1 in both NMP and wild-type retinas, indicating that the NMP protein is able to interact with Rom-1. Retinal samples from $rds^{-/-}$ mice were included as a negative control.

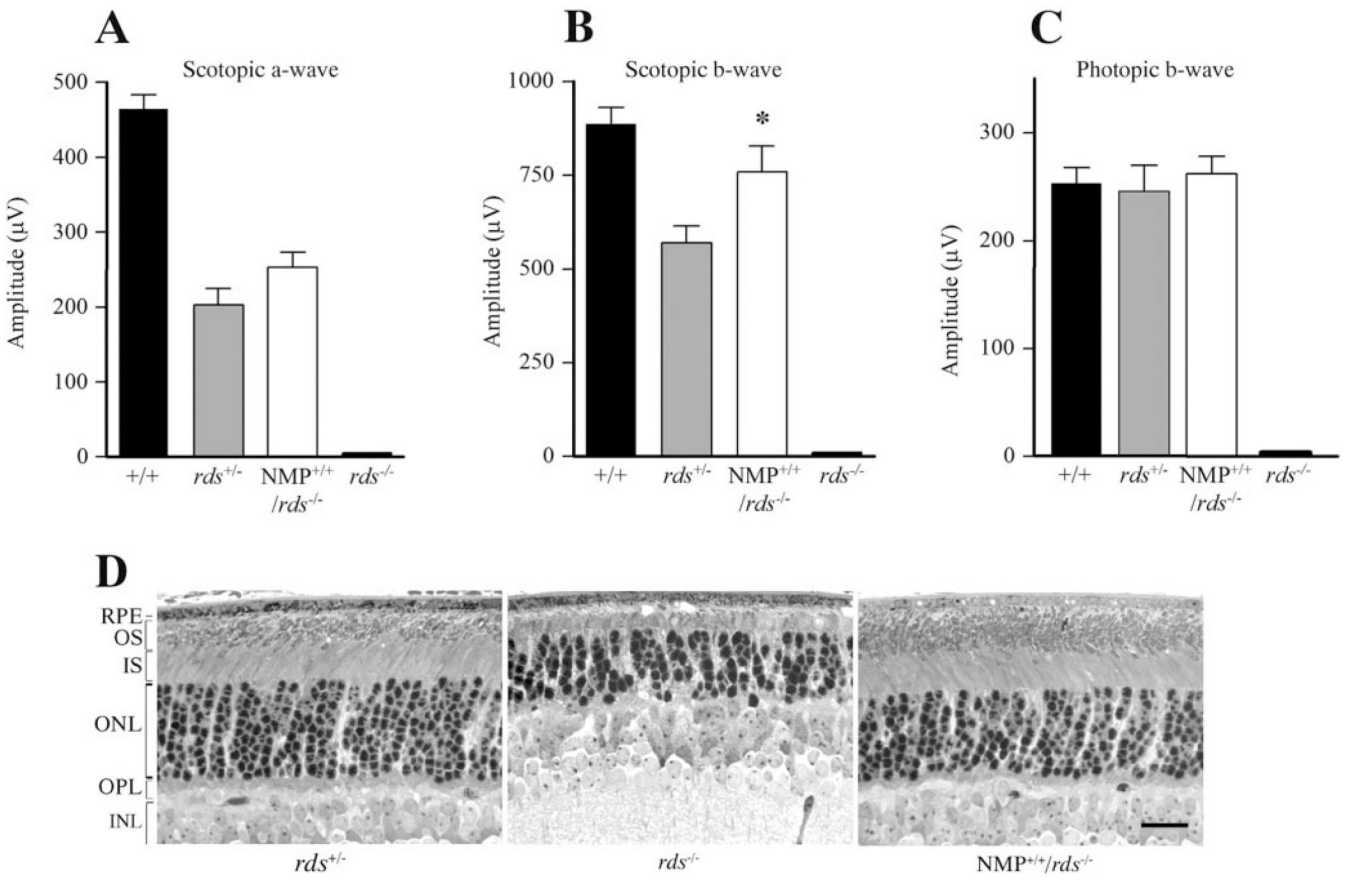

FIGURE 3.

NMP-mediated functional and structural rescue of the $rds^{-/-}$ retina. (**A**, **B**) Scotopic ERG amplitudes show an NMP-mediated restoration of rod photoreceptor function when compared with responses from $rds^{-/-}$. Note that the expression levels of P/*rds* in $rds^{+/-}$ (50% of wild type) and $NMP^{+/+}/rds^{-/-}$ (60% of wild type) correlate well with the increase in scotopic ERG amplitudes. (**C**) Photopic ERG amplitudes demonstrate that one allele of P/*rds* is sufficient to support normal cone photoreceptor function, as revealed by photopic ERG responses from $rds^{+/-}$ and $NMP^{+/+}/rds^{-/-}$ retinas. No rod or cone ERG signal was detected in $rds^{-/-}$ mice. ERG results are an average of 12 to 16 eyes for each genotype at 1 month of age. (**D**) Light microscopy of retinas taken at 30 days of age from $rds^{-/-}$ (*middle*), $NMP^{+/+}/rds^{-/-}$ (*right*), and $rds^{+/-}$ mice (*left*). Note the lack of OS formation in $rds^{-/-}$, whereas a notable improvement in inner and OS structure was seen in $NMP^{+/+}/rd^{-/-}$ retinas. Outer nuclear layer count corresponds to 9 to 10, 6 to 7, and 9 to 10 rows in $rds^{+/-}$, $rds^{-/-}$, and $NMP^{+/+}/rds^{-/-}$ retinas, respectively. Scale bar, 20 μm.

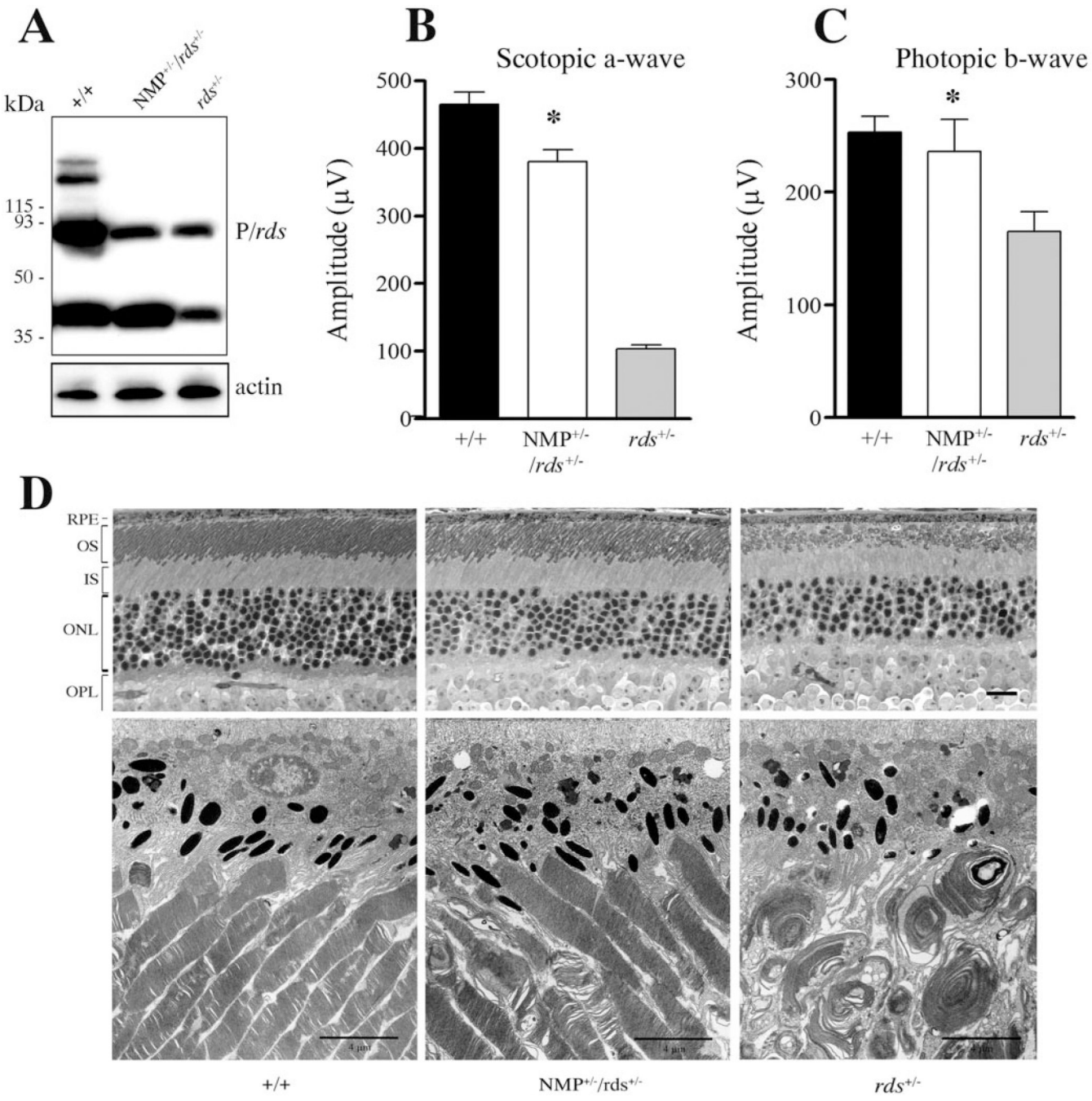

FIGURE 4.

Critical levels of P/*rds* needed for maintaining photoreceptor function and structure. (**A**) Blot analysis demonstrated the increase in P/*rds* protein expression in $NMP^{+/-}/rds^{+/-}$ relative to $rds^{+/-}$ and reflected a level corresponding to 80% of wild type. (**B**) Scotopic and (**C**) photopic ERG analyses at 7 months of age showed a significant improvement in rod and cone ERG amplitudes, respectively, in $NMP^{+/-}/rds^{+/-}$ when compared with $rds^{+/-}$ mice. ERG results are an average of 12 to 16 eyes for each genotype. (**D**) Retinal histology and EM of 7-month-old mice revealed a considerable and long-lasting amelioration in OS structure in $NMP^{+/-}/rds^{+/-}$ relative to $rds^{+/-}$ mice. Light microscopy histology (*top*) shows an outer nuclear layer count

of 9 to 10, 6 to 7, and 5 to 6 rows in wild type, $NMP^{+/-}/rds^{+/-}$, and $rds^{+/-}$ retinas, respectively. *Bottom*: electron micrographs. Scale bar: (**D**, *top*) 20 μm; (**D**, *bottom*) 4 μm.

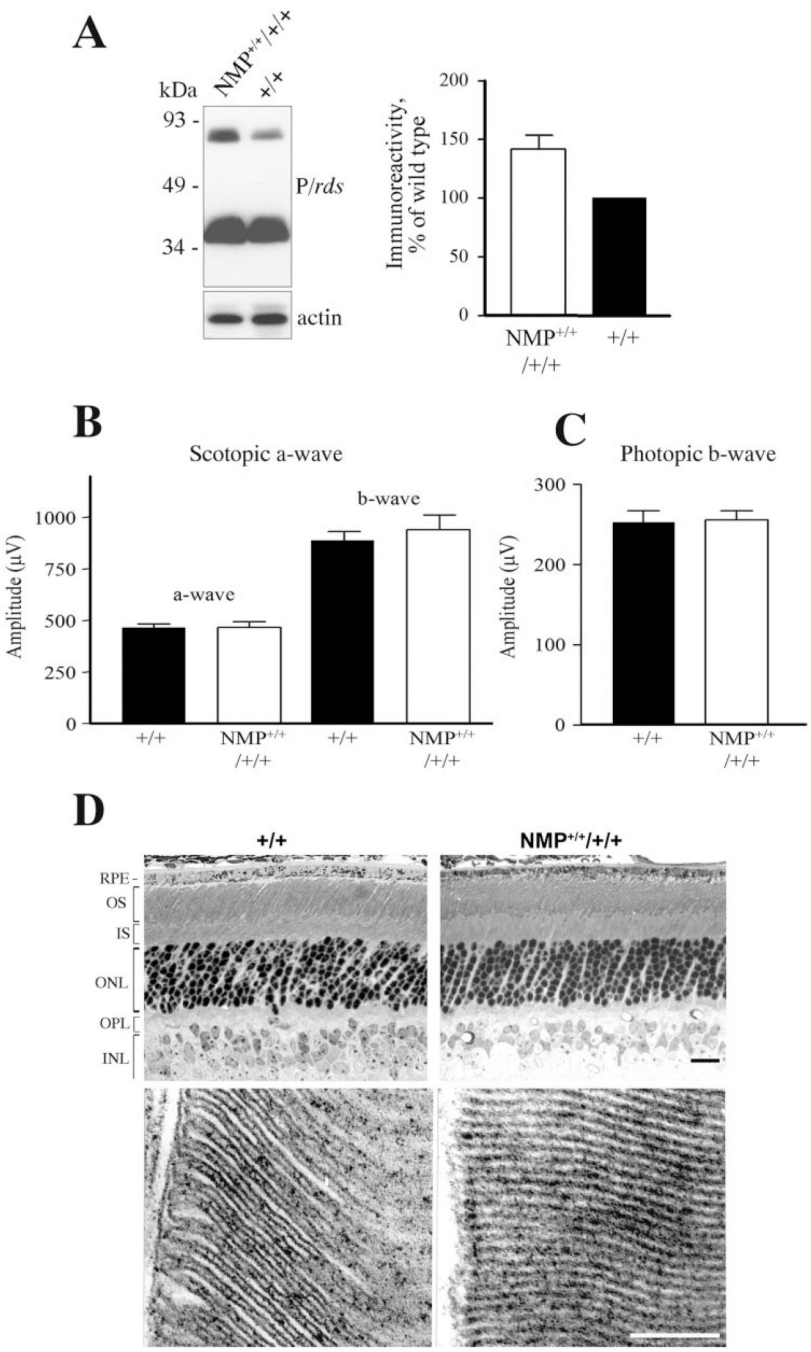

FIGURE 5.

Effect of P/*rds* overexpression on photoreceptor function and structure. (**A**) Blot analysis demonstrated the overexpression of P/*rds* in NMP$^{+/+}$/+/+ retinas relative to wild type. Densitometry scanning of blots revealed a level of P/*rds* equivalent to approximately 150% of wild type. (**B**) Scotopic and (**C**) photopic ERG analyses showed no deleterious effects of P/*rds* overexpression on photoreceptor function up to 7 months of age, the latest time assessed. ERG wave amplitudes represent an average of 12 to 16 eyes for each genotype. (**D**) Histologic and ultrastructural appearances, including outer nuclear layer count (9 – 10 rows), are comparable in retinas from 4-month-old NMP$^{+/+}$/+/+ and wild-type mice, indicating the lack

of negatives effects associated with P/*rds* overexpression in the mouse retina. Scale bare: (**D**, *top*) 20 μm; (**D**, *bottom*) 0.2 μm.